EVALUATING HYDROGEN BLENDING IN COUPLED LARGE-SCALE GAS AND ELECTRICITY NETWORKS

Michele Francesconi*, Carlo Carcasci

Università degli Studi di Firenze, Dipartimento di Ingegneria Industriale, Florence, Italy.

*Corresponding Author: michele.francesconi@unifi.it

ABSTRACT

Sector coupling (SC) strategies, such as utilizing Power-to-Gas facilities to produce hydrogen and injecting it into the existing gas network could offer a rapid and viable approach to decarbonization and managing renewable energy sources (RES) curtailment. Nevertheless, research on real-world large-scale implementation and operational impacts remains limited. This study develops an integrated energy system model for Tuscany (IT), in which hydrogen, produced from curtailed renewable electricity, is injected into the primary high-pressure natural gas transmission pipeline. The main objective is to assess the operational impacts on both the gas and electricity networks and quantify the potential benefits in terms of curtailment reduction and electrolyzer power capacity deployment. The analysis explores two scenarios: the current regulatory hydrogen blending limit in Italy and a comparative scenario with an increased 10% volume threshold. Simulations were performed using the SAInt (Scenario Analysis Interface for Energy Systems) framework, which integrates a transient hydraulic simulation model for the gas network with a quasi-dynamic Alternating Current Power Flow (ACPF) model for the electric system. Our findings indicate that leveraging the main natural gas transmission pipeline can lead to a significant reduction in renewable energy curtailment, with a potential decrease of up to 68% under a 10% hydrogen blending scenario. Additionally, the results show that electrolyzer capacity deployment could reach an average of 41 MW per percentage point of hydrogen volume while ensuring compliance with gas network constraints. However, since hydrogen is not directly sourced from renewable plants, an increase in grid congestion can be observed in the power lines feeding the electrolyzer or in the substations of large renewable power plants due to their higher utilization.

1 INTRODUCTION

Green hydrogen (H_2) production has experienced significant growth in recent years, with a 50% increase since 2021 and projections estimating an annual production capacity of up to 49 million tons by 2030 (IEA, 2024). This trend underscores hydrogen's role as a key energy carrier and an essential flexibility mechanism in high-penetration renewable energy systems, particularly those dominated by solar PV and wind farms, within future low-carbon energy frameworks. During renewable energy overgeneration, surplus electricity can be converted to hydrogen through water electrolysis. This process stores excess energy and serves as a demand-side management strategy, improving overall system efficiency (Vidas et al., 2022). Despite this expansion and the support of preferential investment channels aimed at fostering market adoption, the large-scale deployment of hydrogen technologies remains hampered by critical barriers: the lack of dedicated infrastructure and the high capital and operational costs. Consequently, risk mitigation strategies remain crucial (OECD/World Bank, 2024), both from a technological and policy-making perspective. To de-risk investments, improve infrastructure scalability, and support the widespread integration of hydrogen into the energy system, the coupling of electricity and gas networks, commonly known as sector coupling (SC), presents a promising pathway. Among the various SC strategies, hydrogen blending, which involves injecting hydrogen into existing natural gas network infrastructure, emerges as a viable transitional approach while a dedicated hydrogen infrastructure is being developed (IEA, 2024).

Moreover, it is well established that the physicochemical differences between natural gas (NG) and H_2 introduce technical constraints on feasible blending ratios (BR). High hydrogen concentrations pose significant challenges for existing gas infrastructures, as hydrogen interacts with steel, increasing permeability and causing embrittlement, which in turn raises the risk of pipeline failures (Sofian et al., 2024) (Kappes et al., 2023) (Erdener et al., 2023). Beyond structural concerns, hydrogen blending affects the fluid dynamics of gas transmission, requiring higher volumetric flow rates for an equivalent amount of energy, leading to increased gas velocity, pressure drops, and potential reductions in withdrawal pressure below safe thresholds (Abeysekera et al., 2016). Additionally, it impacts gas quality, modifying key properties such as the Wobbe Index (WI), which is essential for maintaining combustion compatibility and end-use efficiency (Gondal, 2019; Vidas et al., 2022). For these reasons, there is no international standardized regulation on the optimal BR, as it is highly case-dependent.

However, given the extensive capacity of natural gas transmission networks, exceeding 200,000 km in Europe, the injection of hydrogen into major gas transmission pipelines enables, even with modest BRs (below 10% by volume), to accommodate significant quantities of surplus energy that would otherwise be curtailed or rendered economically unviable (Topolski et al., 2022).

Considering this background, we aim to estimate the reduction of curtailed RES energy through hydrogen blending and quantify the average of the additional electrolyzer capacity that can be deployed for a representative dedicated large-scale project. We focus on injecting hydrogen into the main pipeline (MP) rather than at multiple localized points. The analysis accounts for gas network constraints, such as minimal withdrawal pressure and gas velocity limits, and electrical grid constraints, including line loading (LL) and voltage magnitude (VM) at substations.

To date, to the best of the authors' knowledge, several studies have addressed the integration of blending hydrogen as a bulk energy storage and SC strategy with distinct approaches and models: Clegg & Mancarella (2016) analyzed the feasibility of PtG as a seasonal storage solution, developing an integrated electricity-gas model with a steady-state gas flow approach and a Direct Current (DC) power flow model. Cavana et al. (2021) studied electricity-gas network coupling in an urban environment with distributed PV penetration, evaluating hydrogen injection strategies, gas network fluid dynamics, and compositional tracking under different injection locations and blending scenarios. Ekhtiari et al. (2020) developed a steady-state model of the Irish gas network, evaluating the impact of multi-point hydrogen injection from curtailed renewable power over a 24-hour period, emphasizing the variability of hydrogen concentration and the necessity for active gas quality management. Saedi et al. (2021) examined hydrogen integration in the Victorian (Australia) transmission system, developing an integrated electricity-gas system model that combined steady-state optimal gas flow modeling with unit commitment optimization to assess hydrogen blending feasibility on a weekly timescale. Despite these results, this study breaks new ground by uniquely integrating all these characteristics within a single analysis, combining multiple aspects that have been previously considered separately. Specifically, this work:

- Applies a real-world large-scale infrastructure case study with high renewable penetration, focusing on a representative scenario where existing RES plants that have applied for connection to the national grid are considered.
- Applies a quasi-dynamic ACPF simulation for the electricity grid with hourly resolution and a fully transient simulation with hydrogen tracking for gas networks to assess operational impacts.
- Conducts a year-long dual analysis of hydrogen blending limits, evaluating both the maximum percentage allowed by gas transmission system operator (TSO) and an increased BR threshold of up to 10%.

2 MATERIALS AND METHODS

This section details the methodology and materials employed in our study. We first present the simulation parameters and additional equations developed beyond the SAInt (Scenario Analysis Interface for Energy Systems) software framework to enable the co-simulation of electricity and gas networks. Subsequently, we introduce the open data sources used to model network topology and facilities and describe the analyzed scenarios.

2.1 Co-simulation framework

The SAInt simulation platform, a commercially available software developed by encoord (2024), was used for co-simulations. A quasi-dynamic alternating current power flow (ACPF) model for the electrical system was used. Conversely, the gas network is solved using a fully transient hydraulic model. The power flow model determines the steady-state operating conditions of an electrical network by solving nonlinear AC power flow equations. It computes nodal voltages, phase angles, active and reactive power flows, ensuring balance between power generation, demand, and system losses. The model also includes detailed representations of network components, such as transformers and transmission lines. To account for power losses, the fundamental electrical characteristics, including per-kilometer-length resistance, reactance, and susceptance, are calculated by the equations and parameters provided by Karady (2001).
The transient hydraulic model simulates the dynamic behavior of natural gas transport systems by solving the governing partial differential equations of mass and momentum conservation for each pipeline and a mass balance for every node (Pambour et al., 2017). For each gas network node, a minimum pressure constraint is enforced, while for pipelines, both maximum and minimum pressure limits are specified along with key geometrical parameters such as length, diameter, and roughness. Additionally, since the volumetric flow rate ($\dot{Q}_{dmd}$) is insufficient to accurately characterize and describe demand when using varying gas compositions, an energy-based approach was adopted. Hydrogen injection reduces the energy contribution per volume, necessitating gas demand expression in energy terms ($\dot{E}_{dmd}$), as calculated in Eq. (1) which considers the higher heating value of the gas mixture delivered (HHV_g).

$$\dot{E}_{dmd} = \dot{Q}_{dmd} HHV_g \tag{1}$$

After independently simulating the reference scenario for both networks over an entire year, a co-simulation approach is first applied to analyze the gas network scenarios with hydrogen injections. At each hourly step, curtailed energy determines hydrogen production via the electrolyzer facility, which is injected into the gas network according to the allowed hydrogen volume fraction (X_{H2}) in the mixture and volumetric flow rate of the Main Pipeline (Q_{MP}) where the injection occurs (Eq. 2). Following hydrogen injection, the system's dynamic response is evaluated to ensure compliance with the BR constraint ($X_{H2,lim}$). This hard constraint is set and monitored at the node immediately downstream of the injection point. The effective injected hydrogen ($\dot{Q}_{H2,inj}$) is then used to update the electrolyzer electricity demand profile in the new ACPF simulations for each blending scenario, assuming a constant electrolyzer efficiency of η_e=0.6.

$$\dot{Q}_{H2,inj} = \frac{X_{H2} \cdot Q_{MP} \cdot HHV_{NG}}{X_{H2} \cdot HHV_{H2} + (1 - X_{H2}) \cdot HHV_{NG}} \tag{2}$$

To quantify the utilization of curtailed renewable energy for hydrogen production, a Curtailment Utilization Index (*CUI*) is defined, representing the percentage of curtailed energy successfully converted into hydrogen and injected into a gas network over an entire year (8760 hours). This relationship, expressed through two distinct terms in Equation (3), highlights two different operational conditions. The first term represents the total energy converted by the electrolyzer, accounting for its nominal electric power (P_e) and efficiency, over the design operating hours (t_d) in which hydrogen injection remains within the permissible limits. The remaining hours account for the maximum allowable injection in the main pipeline, ensuring compliance with the imposed concentration constraint. The total amount of hydrogen available is calculated from total curtailed renewable power ($P_{c,\,RES}$).

$$CUI = \frac{HHV_{H2}\left[\sum_{t=0}^{t_d} \frac{P_e}{HHV_{H2}} \eta_e \, \Delta t + \sum_{t=0}^{8760-t_d} \frac{X_{H2,lim} \cdot Q_{MP} \cdot HHV_{NG}}{X_{H2,lim} \cdot HHV_{H2} + (1 - X_{H2,lim}) \cdot HHV_{NG}} \Delta t\right]}{\sum_{n=1}^{8760} P_{c,RES} \cdot \eta_e \cdot \Delta t} \tag{3}$$

To provide comparative analysis, assessment of CUI, and the evolution of the system's operational impact, multiple scenarios have been simulated:

- Baseline Scenario (or $X_{H2,lim}$=0%): This scenario is constructed based on Tuscany's existing renewable energy infrastructure, integrating all renewable energy projects currently applied for connection to the national grid considered by the province. Despite the national 2% H_2 limit has been established, no hydrogen injection has occurred.
- Regulatory Compliance Scenario: This scenario reflects the current Italian regulatory limit for the presence of hydrogen in the mixture, which, is $X_{H2,lim}$=2%. It represents a low hydrogen injection case, ensuring compliance with existing legislative constraints. The electrolyzer nominal power needed to ensure the maximum hydrogen injection at the maximum flow rate of the targeted pipeline is P_e=79 MW_{el}.
- Enhanced Hydrogen Blending Scenario: This scenario explores an increased hydrogen blending ratio of up to $X_{H2,lim}$=10%, representing a forced case to assess its technical feasibility, operational challenges, and grid impact compared to the regulatory limit. The electrolyzer nominal power needed to ensure the maximum hydrogen injection at the maximum flow rate of the targeted pipeline is P_e=414 MW_{el}.

2.2 Case study description

A regional energy system model for Tuscany (Italy) was developed using the 2019 infrastructure dataset. The model covers the region's northern gas network (GNET) and the comprehensive electric network (ENET), spanning all ten provinces. These represent the gas withdrawal nodes and the terminal buses of electricity consumption.

2.2.1 Integrated model of coupled electricity and gas infrastructure in Tuscany

The modeled networks include 20 pipelines and 21 nodes for GNET, alongside 47 transmission lines, 47 buses, and 12 transformers for ENET. The key operational nodes, including the highest nominal power plant for each energy source and the critical network elements relevant to the analysis, are presented in Figure 1.

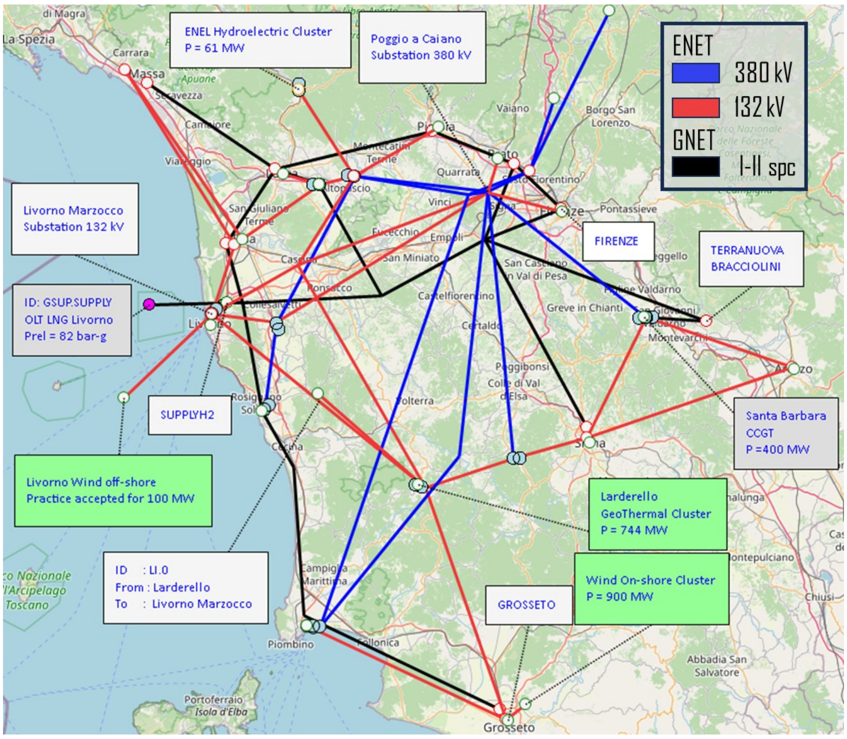

Figure 1: Electric and gas network of Tuscany from SAInt graphical interface with geographic map reference. Circles represent electric buses and gas network nodes, while connections represent electric power lines and gas network pipelines.

The modeled electricity infrastructure consists of 380 kV high-voltage transmission lines and 132 kV high-voltage lines. The gas network is represented by a subset of the high-pressure system (>75 bar-g) in northern Tuscany, including both I-II species for pipelines.

Tuscany was selected for its simplified high-pressure gas infrastructure, which allows for the consideration of a single NG supply, whose injected flow rate is known (Snam 2015). The only natural gas supply node considered is the Offshore LNG Toscana (OLT) terminal in Livorno, which is connected to the mainland via a 28.5 km offshore pipeline. Operating as a Floating Storage and Regasification Unit (FSRU), the terminal maintained an average flow rate of 543.41 kSm^3/h at 82 bar-g (Snam, 2023), with no compressor station. The onshore pipeline directly connected to this injection point is considered the target MP in our model, where the maximum flow rate occurs. Geospatial topology and positioning data of gas stations were obtained from (Snam, 2025), while pipeline diameters and limit pressure values were sourced from (Snam, 2015) and (Snam 2021).

The hydrogen production facility, linking electricity and gas networks, is assumed to be located in Livorno's industrial zone (labeled "SUPPLYH2" in Figure 1). Connected to the “Livorno Marzocca” 132 kV substation and is assumed to inject hydrogen into “SUESE”, the closest technically feasible gas station. The injected hydrogen, produced via electrolysis, is assumed to have a purity of 100% while the natural gas composition corresponds to the LNG specifications from Snam (2021).

For the electric grid, the 132 kV network includes only the essential transmission lines required to connect major load centers, prioritizing clarity and traceability over a full-scale representation. The electrical network model was constructed with geospatial integrity, utilizing facilities exact coordinates data from OpenInfraMap and RSE (2021). The transmission carrying capacity (LL_{max}) at the thermic limit for power lines, calculated according to Italian standards (CEI 11-60, 2002), is determined based on 675 A for the 132 kV lines with a single aluminum-steel conductor per phase and 2310 A for the 380 kV lines with a triple aluminum-steel conductor per phase.

The power generation mix includes all operational plants as of 2019 with capacities exceeding 20 MW, sourced from (RSE, 2021). For simplification, some facilities were aggregated, such as the 744 MW Larderello geothermal complex and northern Tuscany's hydroelectric facilities. The renewable generation scenario includes current RES operational plants and approved projects prioritized for commissioning (Terna, 2025). Since no PV plants are present in Tuscany, provincial-level installed capacities for solar PV were considered (GSE, 2023).

Renewable generation profiles for each province were obtained from the PVGIS database. Solar generation was estimated to be proportionate to irradiance, while wind power to wind speed ($v_{w,ref}$) of PVGIS reference height (h_{ref}). To put the value on a more representative 100-metre height for a wind turbine an adjustment was performed using the power law equation (Eq. (4)), applying an exponential coefficient (k = 0.017) to account for vertical scaling (Deshmukh and Deshmukh, 2008). Finally, the wind turbine power output (P_{WT}) was then computed using Equation 5, where the cut-in ($v_{w,ci}$), rated ($v_{w,r}$), and cut-off ($v_{w,co}$) wind speeds were set at 3 m/s, 13 m/s, and 25 m/s, respectively. Outside this range, for wind speeds below the cut-in and above the cut-off, the power output is considered zero.

$$v_w = v_{w,ref} \cdot \left({h_{WT}}/{h_{ref}} \right)^k \tag{4}$$

$$P_{WT} = \begin{cases} P_{WT,r} \frac{v_w^3 - v_{w,ci}^3}{v_{w,r}^3 - v_{w,ci}^3} \; ; \; v_{w,ci} \leq v_w \leq v_{w,r} \\ P_{WT,r}; \; v_{w,r} \leq v_w \leq v_{w,co} \end{cases} \tag{5}$$

It is assumed instead that the other non-programmable energy sources are only constrained by a maximum ramp rate of 4 MW/min, as a reasonable approximation for operational flexibility.

2.2.2 Energy demand

Both energy systems utilized 2019 hourly demand profiles to maintain infrastructure consistency. For the electricity network, hourly provincial demand profiles were generated using the TOTEM software (RSE, 2023). To account for electric external energy exchanges, the net energy flows between the Central-North (CN) and Central-South (CS) zones (Terna, 2019) were subtracted, resulting in a net virtual electricity demand that better reflects regional consumption dynamics without external supply influences. For the gas network, the average gas demand per province was sourced from (MASE, 2019) and disaggregated by sector, considering domestic, commercial, and industrial uses. To generate hourly demand patterns, synthetic sectoral consumption profiles were derived from Guzzo et al. (2024). Realistic consumption variability was adjusted by applying random noise: 2% for industrial demand and 5% for commercial and residential sectors. Finally, the system is then completed by setting the flow rate injected by the OLT, as an energy demand boundary condition at the interconnection node with the national gas grid ('Terranuova Bracciolini' in Figure 1), dynamically adjusted by subtracting the aggregate load of the provinces. The injected daily gas flow rate was derived from (Snam, 2023) and assumed to be constant on an hourly basis. To prevent inconsistencies due to zero-injection mathematical anomalies, missing values were replaced with the daily average flow rate from the preceding week. The other lower-capacity real external connections to the national gas grid were modeled by imposing boundary conditions that consider net gas demand, excluding the portion allocated to the external connections decreased proportionally based on pipeline transport capacity.

3 RESULTS AND DISCUSSION

3.1 Baseline scenario

The annual ACPF simulation results indicate a total energy generation of 12.45 TWh. Table 1 summarizes the generation mix, with Figure 2 detailing dispatch behavior during peak demand weeks. With renewable energy sources prioritized, geothermal power consistently provides the baseload supply throughout the year. The three thermal power plants, consisting of combined-cycle gas turbines (CCGTs), remain inactive during sufficient renewable energy generation. However, during periods of low RES energy availability, such as on January 19th and January 24th, these CCGT plants activate, balancing both active and reactive power. In this high-renewable penetration scenario, their overall yearly contribution is limited to 14.8%, highlighting the system's reduced reliance on fossil fuels. Furthermore, Figure 2 illustrates a substantial surplus of renewable energy occurring over a significant number of operating hours, highlighting periods of excess generation relative to system demand. Curtailed energy reaches 934 GWh for solar PV and 1001 GWh for wind power, with surplus energy available for 3667 hours annually.

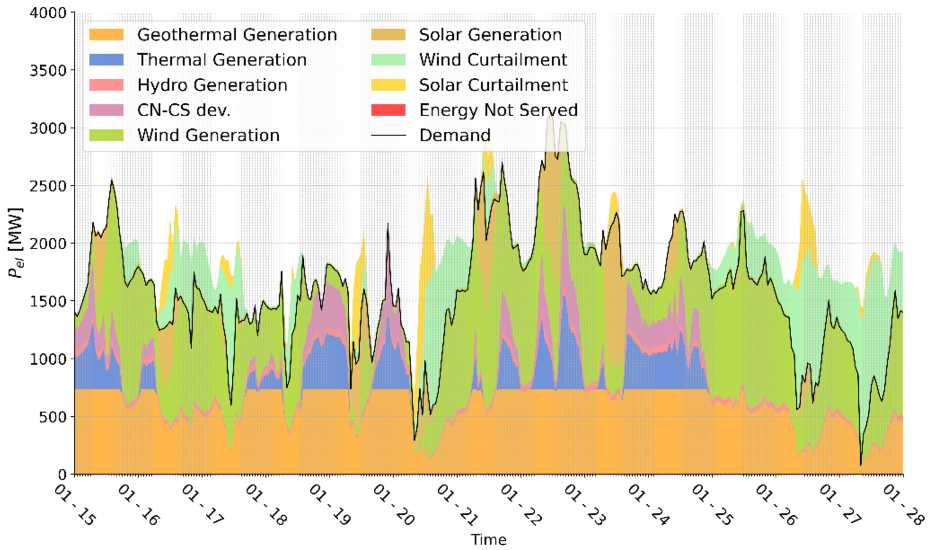

Figure 2: Generation fleet dispatch by generation type and RES curtailments during peak demand.

To further analyze, Table 1 also reports the Deviation from the assumption Centre-to-North and Centre-to-South external exchange (Dev CS-CV). This metric serves as an indicator of the deviation from assumed external exchanges, amounting to just over 10%, reflecting minor discrepancies from expected exchange assumptions. Furthermore, even in the baseline scenario, where no electrolyzer is considered as an electrical load, there are 219 hours in which the electric load limits are exceeded. These violations are analyzed in the next section, where they are directly compared with the other scenarios.

Table 1: Yearly energy generation share by source.

Generation Type	Share of Generation (%)
Natural Gas	14.8%
Solar PV	6.3%
Wind	14.1%
Geothermal	50.1%
Hydro	4.1%
Dev CN-CS	10.6%

Regarding gas network, the total gas delivered throughout the year amounts to 3371 MSm³. To ensure consistency and verify order-of-magnitude estimations, velocity and pressure drop values are evaluated. The minimum pressure is consistently recorded at the farthest node from the injection point ("Terranuova Bracciolini" in Figure 1), with a value of 78.54 bar-g, which is well above the minimum allowable pressure of 75 bar-g at City Gate Stations (CGSs), ensuring network compliance. Similarly, gas velocity remains within standard limits, with a maximum permissible velocity of 25 m/s for I-II species pipelines, while the simulated peak velocity never exceeds 10 m/s. In particular, the highest gas velocity observed (8.15 m/s) occurs in the first downstream pipeline of the MP, which carries the entire injected volume at a constant flow rate while transitioning from an 816 mm to a 512 mm diameter, making it the most critical segment in terms of fluid velocity (Figure 6a).

3.2 Power to Gas scenarios

To facilitate a clearer understanding of hydrogen production and direct injection results, Figure 4 presents a detailed visualization of the simulation outcomes, illustrating the amount of curtailed energy that could be converted into hydrogen, along with the maximum quantities injected into the gas network according to BR constraints during peak demand. The main pipeline volumetric flow rate remains relatively stable with minor variations, while excess RES energy fluctuates significantly, often preventing continuous hydrogen blending.

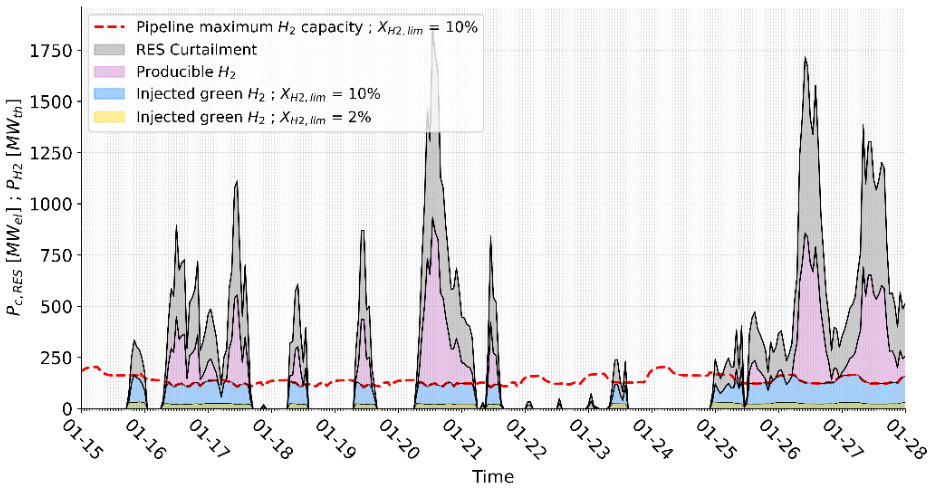

Figure 3: Hydrogen injection and renewable energy curtailment at peak demand.

Different system behaviours can be observed: in some periods, such as between 00:00 on January 22th and 06:00 on January 25th, the 10% limit is sufficient to absorb and fully utilize the available curtailed energy, ensuring complete sector integration. Conversely, in other instances, such as after January 25th, the available renewable surplus is so high that even with the maximum allowable hydrogen injection, some excess energy must still be curtailed.

For a quantitative yearly assessment, Figure 4 shows the load duration curve of CUI, showing that for most of the year, no curtailed energy is available for hydrogen production, with only 3667 hours allowing conversion. On average, for the 2% injection scenario, only 32.5% of the curtailed energy is utilized, whereas for the 10% injection case, the share increases significantly to 68.4%. Statistical indicators are reported for better understanding of coupling capability, such as the second quartile (Q2, median) and third quartile (Q3). Notably, for the 10% H_2 blending scenario, Q3 precisely reaches the threshold value of 100%, whereas in the 2% case, Q3 is significantly lower at 47.9%, less than half. Similarly, Q2 exhibits a significant rise, increasing by more than five times, deviating from a simple proportional trend. Furthermore, the number of hours where the available curtailed energy is fully converted into hydrogen (CUI = 100%) is 1,634 hours out of 3667 for the 10% blending case compared to just 596 hours in the 2% scenario, reinforcing the impact of increasing hydrogen injection limits on energy recovery.

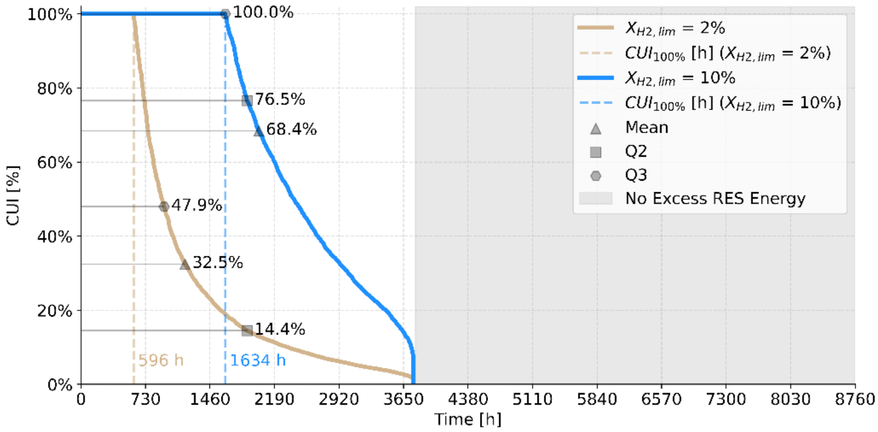

Figure 4: CUI load profiles and statistical metrics for both PtG scenarios.

Lastly, Table 2 summarizes the key performance indicators for the gas-electric system under different hydrogen blending scenarios. These indicators include the Wobbe Index, CO_2 reduction calculated using a natural gas emission factor of 51.4 kg/GJ (Saedi et al., 2021), and the number of hours in which the line loading ratio (Eq. (6)) exceeds 100%. The latter is obtained by summing up the hours of exceedance of each limit for current (I), active power (P), and apparent power (S), calculated as the difference between the baseline case and the simulated case (ΔLL [h]), implicitly assuming that any initial violations result from modeling constraints rather than real energy issues. Additionally, the table reports the electrolyzer installed capacity required per unit of injected hydrogen and the percentage of hydrogen injected per 100 MW of installed capacity.

$$LL_j(\%) = \left(LL/LL_{j,max}\right) \times 100,\ j \in \{I, P, S\} \tag{6}$$

Table 2: Summary results for each $X_{H2,lim}$ scenario

$X_{H2,lim}$ scenario	0%	2%	10%
$MW_e/\%_{vol}$ [-]	-	39.01	42.83
$\%_{vol}$ /100MW_e [-]	-	2.531	2.415
ΔLL [h]	0	49	241
CO_2 reduction [kton/y]	-	0.713	50.98
v [m/s]	8.15	8.29	9.06
p_{min} [bar-g]	78.54	78.47	78.09
WI [MJ/Sm^3]	52.01	51.74	51.47

The average installed power of hydrogen facilities remains nearly constant for each percentage point of injection, demonstrating that there is an ample margin of curtailment reduction of up to 10%.

The main benefit is a significant increase in the number of hours operating at 100% capacity, reducing the time the electrolyzer must operate in off-design conditions. An interesting result emerges in the 2% blending scenario. Since the overall energy demand remains unchanged, the increase in gas flow partially offsets the advantage of hydrogen dilution by slightly increasing the natural gas (NG) content. This nearly eliminates the decarbonization benefits, which are significantly lower than in the 10% case. This is because H_2% is not linearly correlated with the percentage of energy and thus direct CO_2 emissions (Sofian et al., 2024). Conversely, the 10% blending scenario achieves a significantly higher CO_2 reduction, albeit requiring a slightly larger installed capacity (+3 MW_{el}). However, unlike the regulatory compliance scenario, which only slightly increases the number of hours exceeding network limits, this approach quintuples the instances of transmission line overload, demanding more robust network reinforcement measures.

Nevertheless, neither scenario violates gas network constraints, which remains fully capable of accommodating hydrogen injection from both a fluid dynamic and qualitative perspective. Specifically, in the gas network, the observed maximum increase in gas flow velocity (+11.1%) and decrease in pressure drop (-5‰) remain within acceptable operational limits. Likewise, gas quality is only marginally affected, with the Wobbe Index (WI) varying by just 1%.

3.3 Operational impact

3.3.1 ENET

To aid in the interpretation Figure 5a presents the temporal evolution of the most critical constraint violations under different PtG scenarios, focusing on the most stressed power line. The loading conditions of the electrical network, particularly on transmission lines, were showed in terms of current loading (LLI), active power loading (LLP), and apparent power loading (LLS). The maximum constraint breach occurred at 13:00 on January 21th, primarily due to the current exceeding its allowable limit. This critical overload is observed on the 132 kV transmission line connecting the province of "Grosseto" and "Livorno Marzocco" substation. Unlike higher-capacity 380 kV transmission lines, this 132 kV corridor is inherently more susceptible to congestion. These lines are connected to various renewable plants, primarily to the high-capacity (900 MW) wind farm in Grosseto.

Notably, the difference between the baseline scenario and the 2% hydrogen blending case is minimal. However, in the 10% blending scenario, high spikes, reaching up to 126% of the maximum load, are observed. Both line loading and voltage magnitude drop are significantly higher. This phenomenon is further illustrated in Figure 5b, where it can be observed that, at the same critical hour, the voltage level at the node with the highest onshore Wind and PV generation ("Grosseto") experiences an intense drop below 0.95 pu lower limit. These peaks occur during specific hours when greater amounts of RES can be utilized for electrolyzer operation, because the hydrogen production facility is not directly connected to the renewable generation site.

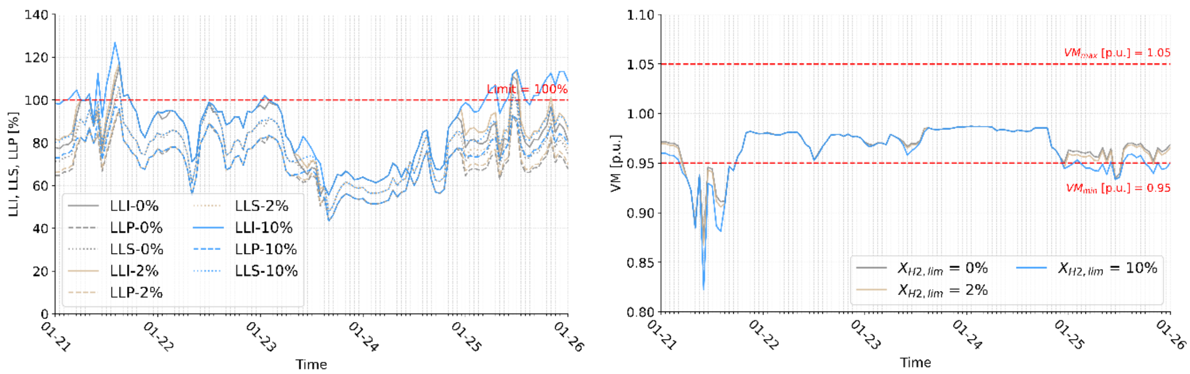

(a) (b)

Figure 5: Line loading for the most critical branch (a) and Voltage Magnitude for the most critical substation (b) Under peak operating conditions.

3.3.2 GNET

The operational parameters are evaluated for all pipelines and at each hourly time step. Figure 6a shows the most stressed pipeline downstream of the hydrogen injection station, while Figure 6b shows the node called 'Terranuova Bracciolini', the farthest point of the network from the NG supply. The integration of hydrogen into the gas network appears to have a limited impact on operational conditions, as the gas velocity and pressure drop increase only moderately for each scenario. The only relevant effect is the increase in both the amplitude and intensity of the oscillations for the 10% BR scenario. Velocity, like pressure, is inherently influenced by the load profile, as evidenced by the alternating behavior observed in Figures 6a and 6b. This effect could be particularly relevant as pressure fluctuations contribute significantly to pipeline aging.

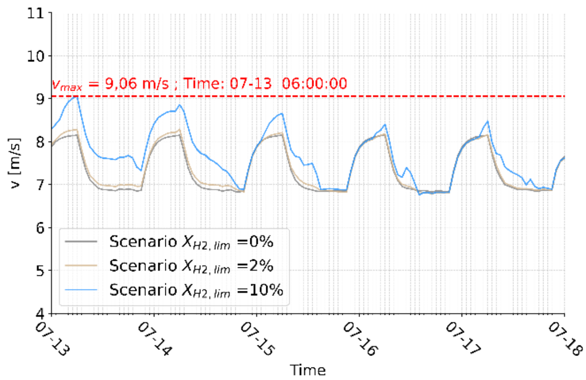

(a)

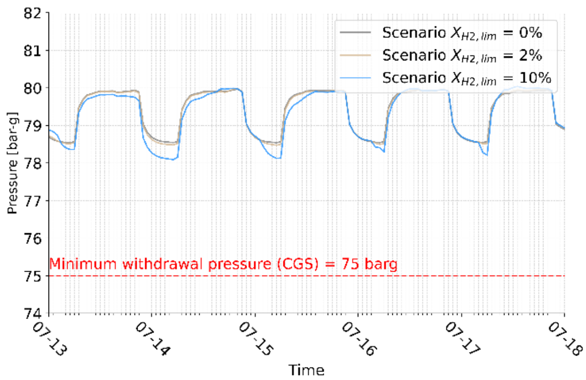

(b)

Figure 6: Maximum gas velocity (a) and minimum withdrawal pressure (b) Detected across GNET under peak operating conditions.

4 CONCLUSIONS

This study develops a geospatially detailed regional gas and electricity system model to evaluate hydrogen blending under high renewable energy penetration. It is considered a single-project hydrogen facility with a direct electrolyzer-to-grid connection and a single injection point into the primary pipeline. The analysis examines operational impacts, decarbonization potential, and large-scale hydrogen production integration. Simulation results indicate that in the low-injection scenario, curtailment reduction and emission mitigation remain modest. However, a large fleet of electrolyzers can be integrated without compromising electricity network stability, positioning hydrogen blending as a key enabler. At higher blending fractions, electrical line loading increases, leading to more frequent operational limit exceedances. Nonetheless, this scenario improves CO_2 mitigation and optimizes infrastructure use, reducing curtailment by up to 68% and fully utilized curtailed energy for more than 1,600 hours annually. Crucially, in both blending scenarios, the high-pressure gas network can totally accommodate the injected hydrogen without constraints. Future research should investigate direct electrolyzer connections to renewable generation sites and assess continuous hydrogen injection strategies, as the primary pipeline has sufficient capacity for higher hydrogen volumes. Additionally, further studies are also needed to evaluate the techno-economic feasibility of large-scale hydrogen blending, particularly regarding the levelized cost of blended hydrogen.

NOMENCLATURE

BR	Blending Ratio	
FRSU	Floating Regasification Unit	
HHV	Higher Heating Value	(MJ/Sm^3)
LLI	Line loading for current	(%)
LLP	Line loading for active power	(%)
LLS	Line loading for apparent power	(%)
MP	Main Pipeline	

P	Power	(W)
p	Pressure	(Pa)
PtG	Power to Gas	
Q	Volume flow rate	(m^3/s)
RES	Renewable Energy Sources	
S	Apparent power	(VA)
SC	Sector Coupling	
t	Time index	
VM	voltage magnitude	(pu)
v	Velocity	(m/s)
WI	Wobbe Index	(MJ/Sm^3)
X	Hydrogen molar fraction	(–)
η	Efficiency	(–)

Subscripts and superscripts

c	curtailed
ci	cut in
co	cut off
d	design
dmd	demand
e	electrolyzer
el	electricity
g	gas
inj	injected
lim	limit
min	minimum
max	maximum
r	rated
std	standard
th	thermal
w	wind
WT	Wind Turbine

REFERENCES

Abeysekera, M., Wu, J., Jenkins, N., Rees, M., 2016, Steady state analysis of gas networks with distributed injection of alternative gas, *Appl. Energy*, vol. 164: p. 991-1002.

Cavana, M., Mazza, A., Chicco, G., Leone, P., 2021, Electrical and gas networks coupling through hydrogen blending under increasing distributed photovoltaic generation, *Appl. Energy*, vol. 290: p. 116764

CEI 11-60, Carrying Capacity at Thermic Limit of Overhead Lines Exceeding 100 kV; CEI: Milan, Italy, 2002.

Clegg, S., Mancarella, P., 2016, Storing renewables in the gas network: modelling of power-to-gas seasonal storage flexibility in low-carbon power systems, *IET Gener. Transm. Distrib*., vol. 10, no. 3: p. 566-575.

Deshmukh, M.K., Deshmukh, S.S., 2008, Modeling of hybrid renewable energy systems, *Renew. Sustain. Energy Rev.,* vol. 12: p. 235-249.

encoord, 2024, Scenario Analysis Interface for Energy System (SAInt), www.encoord.com

Ekhtiari, A., Flynn, D., Syron, E., 2020, Investigation of the multi-point injection of green hydrogen from curtailed renewable power into a gas network, *Energies*, vol. 13, no. 22: p. 6047.

Erdener, B. C., Sergi, B., Guerra, O. J., Chueca, A. L., Pambour, K., Brancucci, C., Hodge, B. M., 2023, A review of technical and regulatory limits for hydrogen blending in natural gas pipelines. *Int. J. Hydrogen Energ.*, vol. 48, no. 14: p. 5595-5617.

Gondal, I.A., 2019, Hydrogen integration in power-to-gas networks, *Int. J. Hydrogen Energy*, vol. 44: p. 1803-1815

GSE, 2023, Solare fotovoltaico – Rapporto statistico 2023, Gestore dei Servizi Energetici, Rome

Guzzo, G., Francesconi, M., Carcasci, C., 2024, Smart management of pressure regulating stations to maximize hydrogen injection in a gas distribution network, Int. J. Hydrogen Energy, vol. 69: p. 626-634.

IEA (2024), Global Hydrogen Review 2024, IEA, Paris, License: CC BY 4.0

MASE, 2021, Ministero dell'Ambiente e della Sicurezza Energetica, "Consumi Provinciali di Gas Naturale", Available from: https://sisen.mase.gov.it/dgsaie/consumi-provinciali-gas-naturale

Karady, G.G., 2001, Transmission system, The Electric Power Engineering Handbook, Ed. L.L. Grigsby, CRC Press LLC

Kappes, M.A., Perez, T.E., 2023, Blending hydrogen in existing natural gas pipelines: Integrity consequences from a fitness-for-service perspective, *J. Pipeline Sci. Eng*., vol. 3: p. 1001411

OECD/The World Bank 2024, Leveraging De-Risking Instruments and International Co-ordination to Catalyse Investment in Clean Hydrogen, Green Finance and Investment, *OECD Publishing*, Paris

OpenInfraMap, Open Infrastructure Map. Available from: www.openinframap.org/#2/26/12.

Pambour, K.A., Cakir Erdener, B., Bolado-Lavin, R., Dijkema, G.P.J., 2017, SAInt – A novel quasi-dynamic model for assessing security of supply in coupled gas and electricity transmission networks, Appl. Energy, vol. 203: p. 829-857.

PVGIS, Photovoltaic Geographical Information System, European Commission, available from: https://re.jrc.ec.europa.eu/pvg_tools/en/

RSE, 2021, Ricerca sul Sistema Energetico, "Atlante Integrato per il Sistema Energetico Nazionale", Available from: https://atlanteintegrato.rse-web.it/.

RSE, 2023, Metodologia di ottimizzazione a molti obiettivi basata sull'utilizzo di indicatori di sostenibilità, Ricerca sul Sistema Energetico, Milan.

Saedi, I., Mhanna, S., Mancarella, P., 2021, Integrated electricity and gas system modelling with hydrogen injections and gas composition tracking, *Appl. Energy*, vol. 303: p. 117598.

Snam, 2015, "Gas network and transport infrastructure – Sections 2, 4, and 5", Available from: www.snam.it/it/i-nostri-business/trasporto/servizi-online/la-rete/rete-gas-e-infrastrutture-trasporto-gas.html.

Snam, 2021, Composizioni dei gas tipici immessi nella rete di trasporto Snam Rete Gas AT2020-2021, internal document, November 14, 2021. Available from: https://misura.snam.it/portmis/coortecDocumentoController.do?menuSelected=4300

Snam, 2023, Dati operativi OLT Offshore LNG Toscana. Available from: www.snam.it/it/trasporto/dati-operativibusiness/4_Dati_operativi_GNL/

Snam, 2025, Mappatura della Capacità di Trasporto Attuale, internal document, Available from: https://www.snam.it/it/i-nostri-business/trasporto/servizi-online/sviluppo-della-rete-e-piano-decennale/procedura-connessioni-biometano.html/.

Sofian, M., Haq, M.B., Al Shehri, D., Rahman, M.M., Muhammed, N.S., 2024, A review on hydrogen blending in gas network: Insight into safety, corrosion, embrittlement, coatings and liners, and bibliometric analysis, *Int. J. Hydrogen Energy*, vol. 60: p. 867-889.

Terna, 2025, Econnextion: la mappa delle connessioni di rinnovabili e accumuli – Richieste di connessione per provincia, Available from: www.terna.it/it/sistema-elettrico/programmazione-territoriale-efficiente/econnextion.

Terna, 2019, Flusso fisico interno – Electricity transmission data, Available from: www.dati.terna.it/download-center#/trasmissione/flusso-fisico-interno.

Vidas, L., Castro, R., Pires, A., 2022, A review of the impact of hydrogen integration in natural gas distribution networks and electric smart grids, *Energies*, vol. 15: p. 3160

ACKNOWLEDGEMENT

The authors acknowledge the encoord team's support and their provision of the essential software licenses that enabled our research.